

# A Non-contact Machine Vision System for the Precision Alignment of mm-Wave Antennas in all Six Degrees of Freedom

\*Joshua A. Gordon, David R. Novotny

Electromagnetics Division, National Institute of Standards and Technology  
Boulder, CO 80305

\*josh.gordon@nist.gov

**Abstract**— Although highly accurate relative position data can be achieved using laser tracking systems which are suitable for millimeter wave antenna characterization, a considerable gap exists in the ability to absolutely align antennas to laser tracker target coordinate systems. In particular this scenario arises in millimeter wave near-field measurements where probe antenna aperture dimensions are on the order of a millimeter, and the position of its origin must be known to better than 1/20th of a wavelength, and orientation known to fractions of a degree. The fragile nature and dimensions of such antenna negate the use of coordinated metrology measurement systems and larger touch probes typically used for accurate spatial characterization. The Antenna Metrology Laboratory at NIST in Boulder, Colorado is developing a new machine vision based technique for measuring the absolute position of small (~1 mm) millimeter wave antenna apertures relative to a laser tracker target coordinate system. A synergy with existing laser tracking systems, this approach will provide a non-contact method for determining the absolute position and orientation coordinate frame of the probe antenna aperture in all six degrees of freedom to within 30-60 microns. This alignment system technique is demonstrated using the CROMMA Facility at NIST in Boulder, CO.

## I. INTRODUCTION

Laser trackers (LT) are effective for the spatial characterization of solid objects and are widely used for spatial metrology tasks such as 3D part characterization, tolerancing, and reverse engineering. They have also been indispensable in advanced surveying applications where high degrees of accuracy and precision are required, such as in aircraft assembly and telescope observatories[1]. LTs have also been useful in the construction and alignment of antenna ranges and antennas [2][3][4]. The type of object that can be spatially characterized with these systems is dependent on the type of LT target used. Perhaps the most common target is the spherical mirror reflector (SMR) made from three perpendicular mirror surfaces forming the corner of a cube. The SMR can be used on its own as a stencil that can be moved along a surface to in a spatial measurement. As typical SMRs are limited to 1" and 0.5" diameter spherical form factor, more complicated targets such as touch probes have been developed to provide increased versatility for manual

scanning of objects allowing for rapid point cloud generation over larger surface areas and volumes.

In the context of precision antenna alignments, LTs are very useful. They allow one to obtain hi-fidelity spatial information at the tens of micron level, which is sufficient for antenna alignments necessary at frequencies in the millimeter-wave (mm-wave) range (100 GHz-300 GHz) [5]. Currently available LT targets are excellent performers for many applications when the object of interest is significantly larger than the target. However, when the object is much smaller than the LT target and too delicate to touch, current LT targets are not adequate. This scenario presents itself regularly when dealing with mm-wave components. As an example, a  $\mu = \pm 1$  probe antenna in the WR-05 waveguide band that would be used in near-field scanning [5] has an aperture of 1.5 mm that is machined to a delicate knife edge. Due to the small size and fragile nature, using an SMR target would not be possible to spatially characterize this probe antenna.



Figure 1. The probe antenna and standard gain horn. Sizes are shown by the ruler.

To address such LT target limitations, the Antenna Metrology Lab at NIST, Boulder, CO has developed a machine vision system. This system uses a set of three cameras in conjunction with LT SMR targets to provide a non-contact method for the spatial characterization and alignment of small mm-wave antennas. It embodies a synergy of machine vision with current LT SMR targets allowing for both the advantages of

spatial mapping and the stand-off nature of optical imaging with laser tracker point-cloud based spatial metrology. With this system, we can measure small and delicate antennas without physical contact to accuracies  $\sim 30 \mu\text{m}$ . In addition, this spatial information is linked to the LT coordinate system, and thus can be incorporated into a broader coordinated metrology framework. In the following sections we will cover the concept, design, function, and example data of this system for precision antenna alignments at 183 GHz at the NIST Configurable **R**obotic **M**illi**M**eter-wave **A**ntenna (CROMMA) facility in Boulder, CO.

## II. CONCEPT

### A. Non-Contact Machine Vision Linked to a Laser Tracker

The basic concept of this approach is to create a point in space that is coincident with both an SMR target and a vision system. This point can then be used as a virtual touch probe and can also be used to reference other spatial information obtained from the vision system to LT coordinate frames. The use of a vision system opens up many possibilities for non-contact spatial characterization of antennas such as: aperture centroiding, aperture detection, fiducial marker locating, and inspection. Previously, we have presented on the use of machine vision for the relative alignment of antennas[6]; however, here we extend the use of machine vision for the absolute alignment of antennas by linking machine vision information to a LT. With this we can precisely locate mm-wave antennas for aligning and positioning, such as in a near-field scanner. Two mm-wave antennas in the WR-05 band are used to demonstrate this approach; a  $\mu = \pm 1$  probe antenna used in spherical near-field scanning and a 24 dBi standard gain horn (SGH). These are shown in Figure 1 against a ruler for size reference.

With the proliferation of CCD and CMOS cameras, it is not hard to find high-end focal plane arrays (FPA) with pixel sizes on the order of a few microns with several megapixel densities. Furthermore, optical lenses with modulation transfer functions (MTF) above a hundred line pairs per mm are also easy to obtain to match these high resolution FPAs. It is therefore rather easy to achieve imaging resolution on the order of tens of microns. However, although this spatial resolution is readily obtained in the image plane transverses to the optical axis (OA), if we look at the spatial resolution along the OA this is dictated by the depth of focus (DOF) of the lens and not pixel resolution. The DOF is the distance over which an object can be shifted along the OA while still remaining in focus. In a ray optics picture this distance can be considered to be zero; however, for a real optical system due to the wave nature of light the DOF is a non-zero value that depends on the ratio of the focal length to lens aperture, i.e., the f-number  $F/\#$ . The DOF for a rotationally symmetric lens can be closely modeled with a

Gaussian beam. Consider the expression for a Gaussian beam generated by a lens, the DOF [7] is,

$$DOF = \frac{8\lambda}{\pi} (F/\#)^2 . \quad (1)$$

If we want to measure the displacement of an object along the OA then we would want a relatively small DOF, such that we could determine the plane of our object to within the error provided by the DOF. From (1) we see that for small DOF we need small  $F/\#$ . However this typically comes at the expense of a needing to bring the object we are imaging close the lens and so also a decrease in image field of view. For instance, a 50X, F/0.9 microscope objective has very good DOF resolution of  $\approx 1 \mu\text{m}$ , but with an object-to-lens distance of only  $\approx 1 \text{ cm}$ , the field of view is  $\approx 50 \mu\text{m}$ . For measuring antennas in practice, we wish to have a respectable working distance ( $>100 \text{ mm}$ ), such that the camera lens does not interfere with the antenna and accompanying mounting hardware, etc. We also wish to have a field of view large enough to image entire antenna components. In contrast to a microscope objective, a typical machine vision lens provides transvers resolution of tens of microns, with a field of view of tens of mm and object-to-lens distance of hundreds of mm, but with a comparatively *long* DOF of several mm. For the system we present here, the camera lens and FPA used allow for roughly a  $30 \mu\text{m}$  pixel resolution across a total FOV of roughly  $3 \text{ cm} \times 3 \text{ cm}$  at a working distance of  $100 \text{ mm}$ .

Therefore, in order to obtain the same spatial resolution along the OA that can be achieved in the image plane, we need a way to break the ambiguity that results from the relatively long DOF.

### B. Three Camera Concept

To address the DOF ambiguity, a three-camera approach is used. Three cameras are oriented such that the optical axis of one camera is projected along the image plane of the others. The orientation of the cameras used is shown in Figure 2. This way a movement along the axis of one camera is seen as a translation in the other two and thus the DOF ambiguity is broken. As such, the FPA of the other two cameras now provide the needed spatial resolution along the OA of the third camera. In this way we achieve spatial resolution in three directions, along the two dimensions of the image plane and along the OA, comparable to that of just the image plane alone. Below we describe the operation and function of this system and present examples of absolute antenna alignments at 183 GHz using the probe antenna and SGH in Figure 1. We have purposely left out specific details of optical system calibration and design as this is out of the scope of this paper, but will be presented in a future paper.

### C. Linking to Laser Tracker

It is desirable to link the spatial information obtained with the vision system to the coordinate system of the LT. To do this, a centroiding algorithm is implemented whereby all three cameras image a 0.5 inch SMR reflector, denoted as SMR0 in Figure 2, and determine its centroid. Each camera then stores the pixel location of this centroid in memory. Five additional SMRs (SMR1 through SMR5) which have a fixed relationship to SMR0, are attached at the base of the cameras. The magnetic nest locations of these are also shown in Figure 2. SMR0 through SMR5 are then captured by the LT forming a constellation of LT points. This is shown in Figure 3.

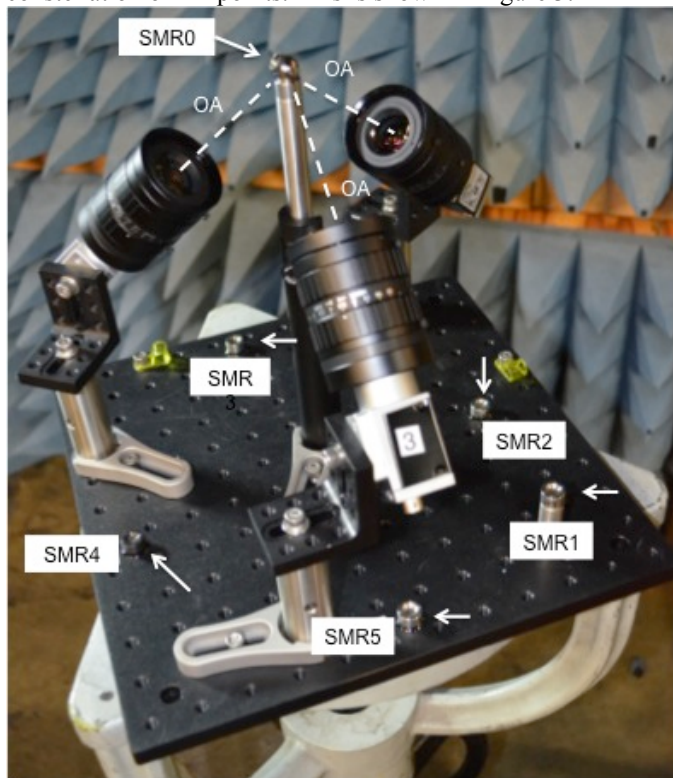


Figure 2. Three-camera vision system showing orientation of camera optical axis (dashed lines), and SMR locations .

Because there is a fixed relationship between SMR0 and SMR1:5, SMR0 is removed and only SMR1:5 need be measured by the LT to deduce the location of SMR0. After removal of SMR0 the pixels for the centroid location of SMR0 that are stored in memory are high-lighted in all the images captured by each camera. When an object appears to lie at the same location as the highlighted centroid pixels *in all three cameras simultaneously*, then that object occupies the same location as centroid of SMR0. This is by virtue of the fact that all three camera’s centroid pixels correspond to the same point in space, the centroid of SMR0. Therefore, we need only to co-locate a feature on an object we wish to measure with these highlighted pixels in the image of all three cameras and measure the positions of SMR1 through 5 to determine the location of that feature in the LT coordinate system. The key

here is that we have linked the location of SMR0 to the LT and the cameras without needing SMR0 to remain physically in place. As such we need only to co-locate the object we want to measure with the highlighted pixels in the camera images and capture the remaining SMRs 1 through 5. In this way we no longer need a physical target to touch the object we are trying to measure with the LT. In essence we have created a virtual LT target that is the size of the field of view of one camera pixel or about 30 microns.

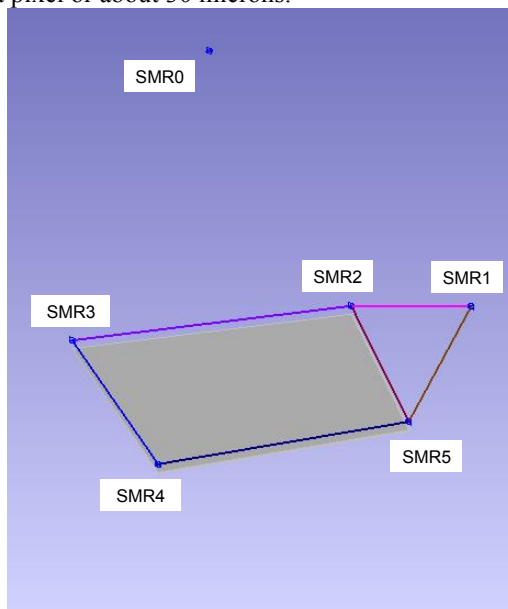


Figure 3. Constellation of LT points corresponding to SMR0 through 5 locations. Lines and plane joining points are shown to help show the reader spatial relationships.

This virtual target is used to “touch” off on points of an object we are trying to measure without ever actually touching it. Combined with machine vision algorithms this allows us to characterize very small antenna components (~1mm) to within tens of microns, yet within a FOV of tens of mm, at working distances of hundreds of mm and over volumes as large as the LT range-typically tens of cubic meters.

The spatial metrology enabled by this system enables us to determine coordinate frames in all six degrees of freedom for these antennas so that precision alignments can be achieved and linked to a LT coordinate system.

## III. FUNCTION

### A. Edge Detection and Centroiding

Using cameras allow us to take advantage of machine vision algorithms for finding antenna features useful for alignments and positioning at the pixel level. Furthermore the scribe marks used for mechanical references that are typically seen in much larger antennas are usually non-existent on mm-wave

antennas. As such using machine vision algorithms allows us to define mechanical references based on the entire antenna aperture itself. Here we demonstrate the use of such algorithms in conjunction with our LT linked camera system to locate and register antenna features from which an antenna coordinate system can be constructed. In this machine vision mode, two algorithms are used: 1) edge detection and 2) centroiding, which have proven useful for mm-wave antenna alignments in the NIST CROMMA facility. Many image processing software packages exist today that allow for various edge detection process. All three camera images are scanned to determine the pixel coordinates of antenna aperture edges. From the ensemble of edge pixel coordinates, the centroid of the antenna aperture is determined from a center of mass calculation. The centroid of the aperture is a cardinal point for the center of the antenna aperture and can be used to define the antenna coordinate system.

The edge detection and centroiding process for determining the center of the  $\mu = \pm 1$  probe in the LT coordinate system is described next. In Figure 4, the aperture centroid determined from the edge detection process is represented as the center of the yellow circle. The green boundary defines the region of interest for edge detection. The center of the blue circle is the location of the center of SMR0 stored in pixel memory and known by the LT via the constellation of SMR1:5 (as described above in I.I.C). To determine the centroid of the aperture in the LT coordinate system, the aperture centroid (yellow circle) is co-located with the center of SMR0 (blue circle) in all cameras at the same time, see Figure 5. At this moment the LT captures SMR1:5. Because the center of the aperture occupies the same point in space as the center of SMR0, we immediately deduce the location of the aperture center relative to the constellation of LT points measured from SMR1:5. The absolute location of the centroid is then known in the LT coordinate system to within ~30 microns.

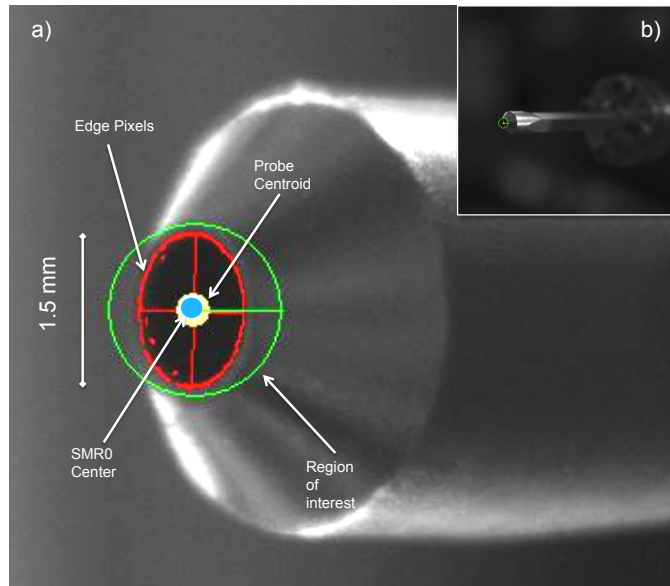


Figure 4. Zoomed in (a) and full FOV (b) images of WR-05 probe. Edge detect pixels (Red), probe centroid (Yellow), SMR0 center (Blue), and region of interest (Green) are shown.

The error in the alignment between the yellow and blue circles can also be determined in real-time from calculating the pixel offset from the center of each circle. This can be done at the sub-pixel resolution using pixel interpolation. Beyond knowing the centroid in the LT frame, we have the added utility that we can now register this centroid to any other LT target in our system. For example, if we wish to track the probe antenna while it is moving, we need only then measure a target that is fixed in position relative to this centroid. This technique is used to precisely locate and track the probe antenna while it is attached to the end of the moving robotic arm in the CROMMA facility. This system is also used for teaching the robot arm the centroid location. This allows the probe antenna to be used as the end effector in the robot kinematic model and aids in antenna probe positioning during near-field scans. The robot teach process is shown in Figure 6, where the robot arm brings the probe centroid into alignment with the location of the center of SMR0 (depicted by arrow) at several different orientations or poses (a)-(d).

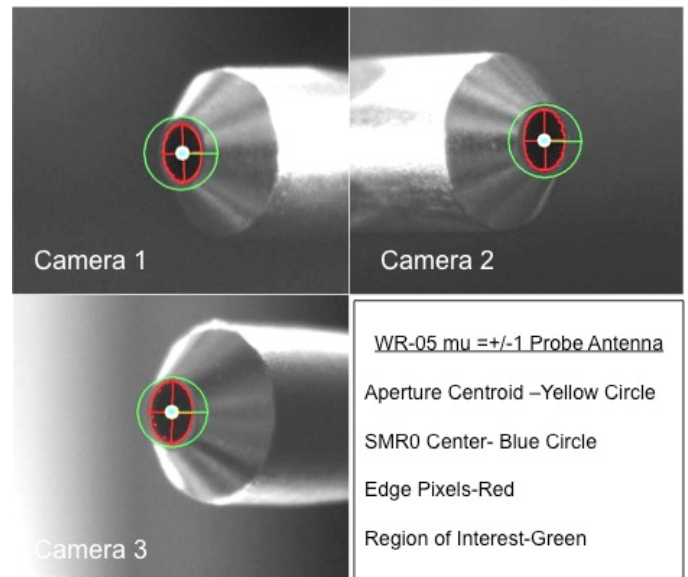


Figure 5. Simultaneous alignment of probe antenna centroid shown in all three cameras. Edge detect pixels (Red), probe centroid (Yellow), Center of SMR0 (Blue), and region of interest (Green) are shown.

### B. Virtual Touch Probe Mode

The method described above for locating the centroid of the aperture in the LT coordinate system does not also allow for the edge of the aperture to be located in the LT coordinate system. This is because the edge points used in determining the centroid are not measured directly in the LT frame of reference. This is in contrast to the aperture centroid, which was co-located with SMR0. Being able to measure the aperture edge is desirable for establishing a plane of reference for the antenna that can be used to define its orientation. We therefore extend this technique so that we can accurately

measure and determine the orientation of the aperture planes of small (~1mm) and larger (>10mm) antennas. We refer to this mode of operation as virtual touch probe mode. In this mode the virtual point defined by the center of SMR0 is used as one would use a physical touch probe, to touch off on a series of locations on an object so that the topology of that object can be determined in the LT coordinate system.

This mode of operation provides flexibility for determining absolute antenna dimensions, tracing out complex shapes, and registering alignment markers to within the 30 micron system resolution. An example of this is shown in Figure 7, where we have traced out the aperture of a the  $\mu = \pm 1$  probe antenna. These data were obtained by using the robot arm to bring the probe aperture to the virtual touch probe point at several locations around its perimeter, and capture these locations with the LT. From these points, a circle fit was performed to determine the aperture diameter and plane orientation relative to the LT tracker target on the robot arm. Through this method, the diameter was determined to be 1.486 mm with an RMS fit error to an ideal circle of 22 microns. Furthermore, from the ideal circle fit, the planarity of probe aperture was determined to be within  $\pm 30 \mu\text{m}$ . This is consistent with design specification of a 1.5 mm diameter and demonstrates the level of precision and accuracy of this technique for measuring small antennas. It also demonstrates an ability to inspect and quantify the mechanical tolerances of such small antennas.

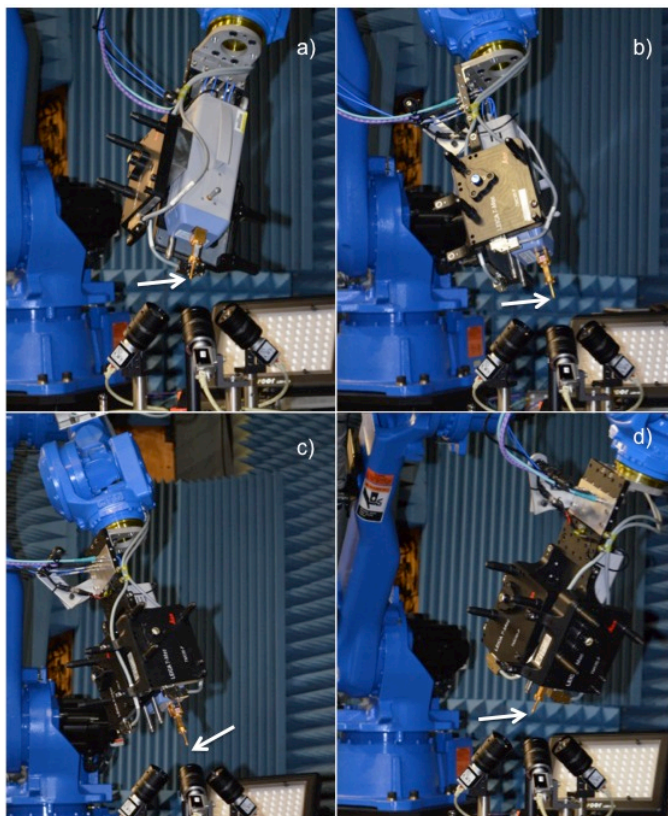


Figure 6. Teaching the location of the probe antenna centroid to the robotic arm in the CROMMA facility through poses (a)-(d).

Similarly we also demonstrate measuring the aperture of the SHG shown in Figure 1 using virtual touch probe mode. An image of this antenna captured with the vision system is shown in Figure 8. Zoomed-in images of each corner are also shown. The arrows in these images show the location of virtual point used to “touch” off at the corners of the SGH. Line segment fits were then made to these corner points from which, the center, plane, and orientation of the was determined. It should be pointed out that a centroiding algorithm, similar to that used for the circular aperture, could have been used, but for a rectangular aperture it is simpler to use virtual touch probe mode.

Upon inspecting the SGH in the cameras, it was apparent that the wall thickness was not consistent and that the internal corners were rounded off and did not define the intersection of the wall edges. As such the blue dots in Figure 8 lie slightly inside the corners at the *effective* location where the walls intersect. This brings up the issue of the stringent mechanical tolerances needed on mm-wave components. In addition, having micro-machined scribe marks, such as can be achieved with laser etching, on such antennas would be beneficial and aid in alignment.

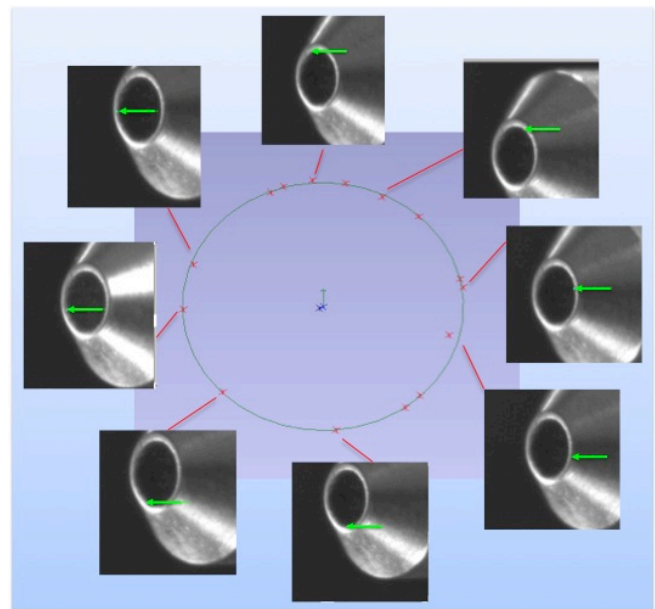


Figure 7. Measured points around the perimeter of the probe aperture using virtual touch probe mode. Arrows show location on probe. The measured diameter measured was 1.486 mm with an RMS error of 22 microns.

If for example a set of micro-machined marks existed on this SHG they would provide a repeatable set of locations to touch off to. This would help repeatability between alignments as well as intercomparison measurements because there would be clear agreement on alignment locations. With this camera system one can easily detect mechanical imperfections on the tens of micron level. Such imperfections become significant for mm-wave antennas because they approach the size of the operating wavelength. Without well defined mechanical reference locations, the mechanical uncertainty due to these imperfections does not allow one to use the geometry of the

component alone for alignment. This allows room for inconsistency between alignment measurements and could possibly affect agreement in antenna performance during intercomparisons. Using the touch probe mode, the length of each side of the SGH was determined to be 12.65 mm X 9.68 mm X 12.63 mm X 9.68 mm. These values are nominally consistent with the manufacturer specifications of 12.55 mm x 9.58 mm.

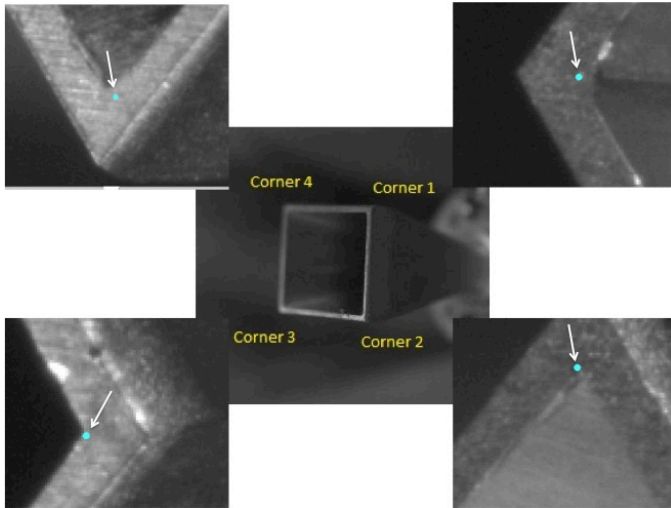


Figure 8. SGH corner measurements using the touch probe mode. Touch probe locations are shown in zoomed-in images by arrows (blue dots).

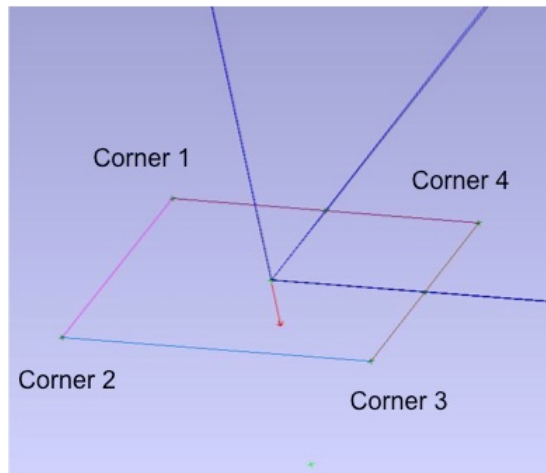


Figure 9. SGH plane and frame constructed from aperture corner locations that were measured with virtual touch probe mode.

#### IV. 6 DOF ALIGNMENT OF ANTENNAS

Combining the aperture centroiding and aperture plane measurement capability of this system, we can readily construct a coordinate system (frame) for each antenna. This frame defines the pose of the antenna in all 6 degrees of freedom (orientation and location) in the LT coordinate system. The frame origins can be constructed from centroid

locations, and frame orientation defined by the plane of the aperture. By virtue of these frames being linked to the LT, we can now track the frame of the 1.5 mm aperture probe antenna relative to the SHG, thereby perform alignments between them to within 30 microns in real time.

#### V. CONCLUSION

In this paper we present a machine vision method for the absolute alignment of mm-wave antennas within a laser tracker coordinate system. The fragile nature and dimensions of these small (~1mm) antennas negate the use of coordinated metrology measurement systems and larger touch probes for accurate spatial characterization. Developed at The Antenna Metrology Laboratory at NIST in Boulder, Colorado this machine vision based technique uses a synergy of three cameras linked to a laser tracker to provide a non-contact method for determining the absolute position and orientation coordinate frame of the probe antenna aperture in all six degrees of freedom to within 30-60 microns. This alignment technique is demonstrated using the CROMMA facility at NIST in Boulder, CO. The concept, design, and function of this system are discussed. Example data for precision antenna alignments are presented, where we show how this system can be used for defining the coordinate systems and aligning a WR-05,  $\mu = \pm 1$  probe antenna and 24 dBi gain standard gain horn operating at 183 GHz in all 6 degrees of freedom.

#### REFERENCES

- [1] A. Rakich, "Alignment of LBT optics using a laser tracker", *Proc. SPIE* 7733, Ground-based and Airborne Telescopes III, 77335K, August 2010
- [2] A. Leon-Huerta, et. al., " Alignment of a large outdoor antenna surface using a laser tracker ", *Proc. SPIE* 8788, Optical Measurement Systems for Industrial Inspection VIII, 878839 May 2013
- [3] G. Hindman, A. Newell, L. Dicecca, and J.C. Angevain, "Alignment Sensitivity and Correction Methods for Millimeter- Wave Spherical Near-Field Measurements"; *2010 Proceedings of the Antenna Measurement Techniques Association*; pp. 316–321; 2010.
- [4] P. Rousseau, W.C. Wysock, and C.M. Turano, J.R. Proctor, "Using a Tracking Laser Interferometer to Characterize the Planarity of a Planar Near-Field Scanner"; *2002 Proceedings of the Antenna Measurement Techniques Association*; pp. 501–506; 2002.
- [5] M. H. Francis, R. C. Wittmann, in "Modern Antenna Hand Book", C. A. Balanis, Chp. 19, 929, 2008
- [6] J. A. Gordon, D. R. Novotny, "Simultaneous Imaging and Precision Alignment of Two mm Wave Antennas Based on Polarization-Selective Machine Vision", *IEEE Trans. Inst. Meas.* vol. 61, pp. 3065-3071, November 2012
- [7] J. E. Greivenkamp "Field Guide To Geometrical Optics", SPIE, Bellingham, WA 2004, pp. 3